

Dalton Transactions

Accepted Manuscript



This is an *Accepted Manuscript*, which has been through the Royal Society of Chemistry peer review process and has been accepted for publication.

Accepted Manuscripts are published online shortly after acceptance, before technical editing, formatting and proof reading. Using this free service, authors can make their results available to the community, in citable form, before we publish the edited article. We will replace this *Accepted Manuscript* with the edited and formatted *Advance Article* as soon as it is available.

You can find more information about *Accepted Manuscripts* in the [Information for Authors](#).

Please note that technical editing may introduce minor changes to the text and/or graphics, which may alter content. The journal's standard [Terms & Conditions](#) and the [Ethical guidelines](#) still apply. In no event shall the Royal Society of Chemistry be held responsible for any errors or omissions in this *Accepted Manuscript* or any consequences arising from the use of any information it contains.



Dalton Transactions

COMMUNICATION

High-Efficiency Bulk Heterojunction Memory Devices Fabricated Using Organometallic Halide Perovskite:Poly(*N*-vinylcarbazole) Blend Active Layers

Received 00th January 20xx,
Accepted 00th January 20xx

DOI: 10.1039/x0xx00000x

www.rsc.org/

Cheng Wang, Yu Chen*, Bin Zhang, Shanshan Liu, Qibin Chen, Yaming Cao, Sai Sun

Dedicated to Professor Dr Michael Hanack on the occasion of his 84th birthday

ABSTRACT: A solution-processed organometallic halide perovskite-based bulk heterojunction (BHJ) memory device with a configuration of indium-doped tin oxide (ITO)/CH₃NH₃PbI₃:PVK/Al has been successfully fabricated. Under a threshold voltage of -1.57 V, this device shows a nonvolatile write-once read-many-times (WORM) memory effect, with a maximum ON/OFF current ratio exceeding 10^3 . In contrast, the ITO/CH₃NH₃PbI₃/Al device showed only conductor characteristics, while the PVK-based device exhibited insulator behavior. Upon being subject to voltages, an interesting filamentary nature of the CH₃NH₃PbI₃:PVK film was also observed in situ at the microscopic nanometer level using a conductive atomic force microscopy (C-AFM) technique with a device configuration of Si/Pt/CH₃NH₃PbI₃:PVK/Pt. The mechanism associated with the memory effect was discussed. The electric-field-induced intermolecular charge transfer effect between CH₃NH₃PbI₃ and PVK, and possible conformational ordering of the PVK side-chains/backbone under an applied bias voltage, may cause the electrical conductivity switching and WORM effect in the reported BHJ device.

Since the first application of an organometallic halide perovskite^{1,2} (CH₃NH₃PbI₃) in dye-sensitized solar cells in 2009,³ this material and its derivatives (e.g. (C₄H₉NH₃)₂(CH₃NH₃)_{x-1}Sn_xI_{3x+1}, CH₃NH₃PbBr_xCl_{3-x}, CH₃NH₃PbBr_xI_{3-x}, CH₃NH₃MX₃ (M = Pb, Sn; X = Cl, Br, I), CH₃NH₃PbCl_xI_{3-x} and CH₃NH₃SnBr_xI_{3-x}) have attracted a growing amount of attention⁴⁻⁷ worldwide in the fields of organic photovoltaics, photodetectors, photocatalysts, transistors, and light-emitting diodes due to their high linear absorption coefficient (1.5×10^4 cm⁻¹ at 550 nm),⁸ tunable bandgap (1.17–2.3 eV),^{6,9,10} long exciton diffusion length (100–1000 nm),^{11,12} high electron

mobility (e.g. 66 cm² V⁻¹ s⁻¹ for CH₃NH₃PbI₃ and 2320 cm² V⁻¹ s⁻¹ for CH₃NH₃SnI₃),¹³ high crystallinity and solution processability. A significant certified power conversion efficiency of 20.1% has been reported so far.¹⁴ Our current interest in perovskites mainly involves their potential applications in memory devices. Some inorganic perovskites with the chemical formula ABX₃, in which the size of cation A is larger than that of cation B, and X is an anion that bonds to both cations, have been used in the fabrication of resistive random access memory devices.^{15,16} However, these high-temperature-processed materials with rigid structures are more breakable during device fabrication and performance measurements.¹⁷ Very recently, Yoo et al. reported the bistable resistive switching effect of a sandwich-type Au/CH₃NH₃PbCl_xI_{3-x}/FTO (fluorine-doped tin oxide) device, with a very small ON/OFF current ratio of ~ 5 and a small turn-on voltage of less than 1 V.¹⁸ Although too small ON/OFF ratio will greatly restrict the practical applications of the corresponding digital devices, this is undoubtedly the first example of hybrid perovskite-based memory devices.

The bulk heterojunction (BHJ) concept has been widely used for mainstream polymer solar cells, in which an interpenetrated charge channel connecting the two electrodes was formed by blending of the polymer as an electron donor with electron acceptor material.^{19,20} The driving force for the charge transport was ascribed either to the concentration-gradient-induced diffusion or the electric-field-induced drift of charge carriers.²¹ In this contribution, using CH₃NH₃PbI₃:poly(*N*-vinylcarbazole) (PVK) for the blend active layers, a solution-processed halide perovskite-based BHJ memory device was fabricated for the first time (**Figure 1a**). Under a threshold voltage of -1.57 V, this device exhibited a nonvolatile WORM memory effect, with a maximum ON/OFF current ratio exceeding 10^3 . The relatively high ON/OFF current ratio can promise a low misreading rate through the precise control of the ON and OFF states, making the device work more high-efficiently. In contrast, the ITO/CH₃NH₃PbI₃/Al device showed only conductor characteristics, while the ITO/PVK/Al device exhibited insulator behavior under the

Key Laboratory for Advanced Materials, School of Chemistry and Molecular Engineering, East China University of Science and Technology, 130 Meilong Road, Shanghai 200237, China. Email: chentanguy@yahoo.com

same experimental conditions. WORM memory, which can be turned ON (high conductivity state) once only and cannot be switched OFF (low conductivity state) even if a reverse bias is applied, usually used in conventional programmable read-only memory devices and also for DVD-R and CD-R media.

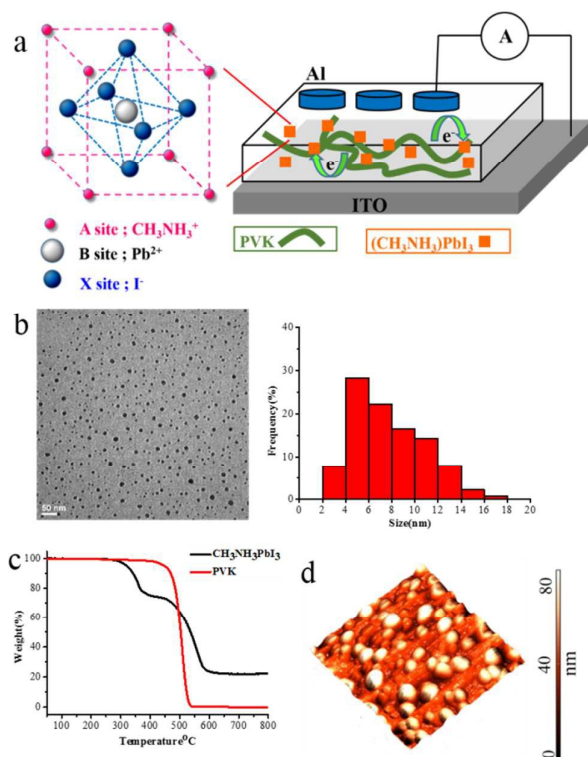


Figure 1. (a) Device structure of the as-fabricated Al/ $\text{CH}_3\text{NH}_3\text{PbI}_3$:PVK/ITO BHJ memory; (b) Transmission electron microscopy image and size distribution of $\text{CH}_3\text{NH}_3\text{PbI}_3$; (c) Thermogram of the samples measured in purified nitrogen; and (d) AFM image of the $\text{CH}_3\text{NH}_3\text{PbI}_3$:PVK film on the ITO substrate.

PVK ($M_w \sim 90\,000$) was purchased from Aldrich Co. The perovskite $\text{CH}_3\text{NH}_3\text{PbI}_3$ was prepared as described by Im et al.⁸ From **Figure 1b**, it can be clearly seen that the diameter of the $\text{CH}_3\text{NH}_3\text{PbI}_3$ crystals was between 2 and 18 nm. Its average diameter was about 7.94 nm. Thermogravimetric analysis of $\text{CH}_3\text{NH}_3\text{PbI}_3$ (**Figure 1c**) indicated two weight-loss plateaus. At lower temperatures, almost no weight loss occurred. Its onset temperature for thermal bond cleavage was 334°C, which is lower than that of PVK (480°C). Atomic-force microscopy (AFM) of the blends showed a roughness of 13.2 nm (**Figure 1d**): a smooth interface at both material/metal contacts can effectively enhance charge injection and transport in the corresponding device. In a typical fabrication procedure for a BHJ memory device, the $\text{CH}_3\text{NH}_3\text{PbI}_3$:PVK (weight ratio: 1:1) active layer (~ 200 nm) was spin coated on the pre-cleaned ITO substrate from a homogeneous γ -

butyrolactone solution of these two components at a spinning speed of 400 rpm for 12 s and then 2000 rpm for 40 s. Afterwards, the device was thoroughly vacuum dried at 80°C overnight. To complete fabrication of the device, Al top electrodes (200 nm thick) were thermally deposited on the surface of the active layer through a shadow mask at 10^{-7} torr. All electrical measurements in this work were performed using a Keithley 4200 semiconductor parameter analyzer in ambient conditions without any protection. The sweeping step was 0.01 V. For comparison, ITO/ $\text{CH}_3\text{NH}_3\text{PbI}_3$ /Al and ITO/PVK/Al devices were also fabricated under the same experimental conditions. An atomic force microscopy (Dimension V, Veeco) equipped with a conducting cantilever coated with Pt was employed for the C-AFM measurements of the device.

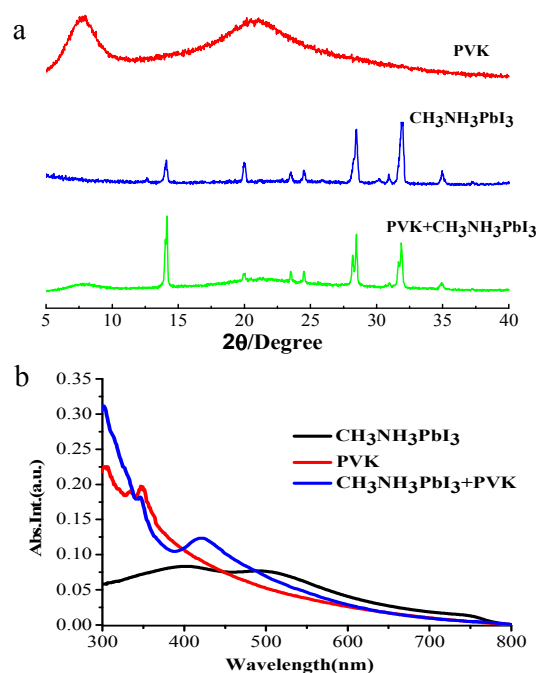


Figure 2. (a) XRD patterns and (b) UV/Vis absorption spectra of the film samples

As shown in **Figure 2a**, the X-ray diffraction (XRD) pattern of PVK had a strong diffraction peak at $2\theta = 7.67^\circ$, from which the nearest chain-to-chain distance was calculated to be 11.51 Å, and a broad, diffuse amorphous halo at $2\theta = 20.64^\circ$ ($d = 4.30$ Å). $\text{CH}_3\text{NH}_3\text{PbI}_3$ has a typical tetragonal perovskite structure,^{22,23} whose characteristic diffraction peaks were found to be centered at $2\theta = 14.1^\circ$ (110), 20.0° (112), 23.6° (211), 24.5° (202), 28.4° (220), 32.0° (310) and 35.0° (312). The corresponding crystal faces are indicated in parentheses. As expected, the XRD pattern of $\text{CH}_3\text{NH}_3\text{PbI}_3$ /PVK blends was a simple superposition of the XRD patterns of these two components. No additional information is available. The UV/Vis absorption spectra of the thin-film samples were

recorded on a Shimadzu UV-2450 spectrophotometer. As indicated in **Figure 2b**, the absorption peaks of the PVK and $\text{CH}_3\text{NH}_3\text{PbI}_3$ films were located at 304, 335 and 347 nm for the former and 402, 503, and 749 nm for the latter, respectively. After blending of PVK with $\text{CH}_3\text{NH}_3\text{PbI}_3$, a new peak at 422 nm was observed in the electronic absorption spectrum of the $\text{CH}_3\text{NH}_3\text{PbI}_3$:PVK film when compared with PVK and $\text{CH}_3\text{NH}_3\text{PbI}_3$.

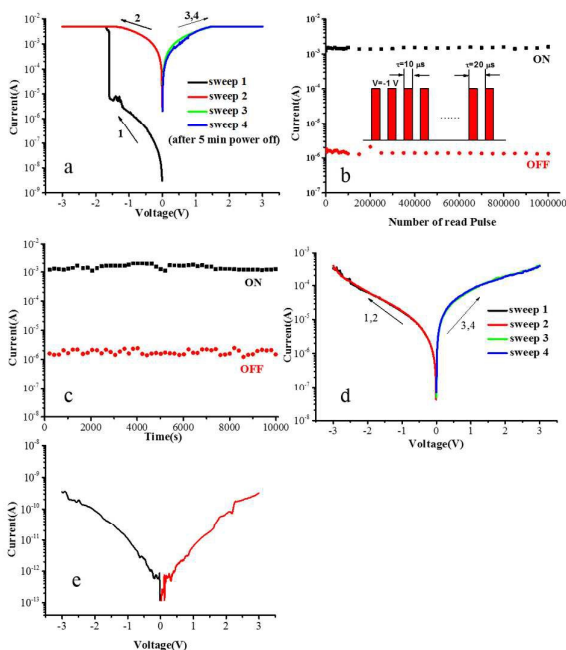


Figure 3. (a) I - V characteristics of the $\text{Al}/\text{CH}_3\text{NH}_3\text{PbI}_3$:PVK/ITO device; (b) Device stability in the ON and OFF states under a continuous read pulse with a peak voltage of -1 V, a pulse width of 10 μs , and a pulse period of 20 μs (the inset shows the pulse used for measurement); (c) Device stability in the ON and OFF state under a constant stress of -1 V; (d) Conductor characteristics of the $\text{Al}/\text{CH}_3\text{NH}_3\text{PbI}_3$ /ITO device; and (e) Insulator characteristics of the $\text{Al}/\text{PVK}/\text{ITO}$ device.

Typical nonvolatile WORM memory behavior obtained from the current-voltage (I - V) profile of the $\text{Al}/\text{CH}_3\text{NH}_3\text{PbI}_3$:PVK (200 nm)/ITO device in an atmospheric environment is shown in **Figure 3**. Generally, a nonvolatile memory device will retain all stored data even if the power is switched off. Initially, as shown in **Figure 3a**, the device was in the OFF state. The current increased slowly along with an increase in the voltage when a negative voltage applied. In this state, the current was rather low. When the threshold voltage of -1.57 V was reached, the current increased suddenly from 10^{-6} to 10^{-3} A. This suggested that the device transitioned from the OFF state to the ON state. Generally, this procedure served as the writing process. The ON state device retained its high conductivity state in the following forward- and reverse-biased sweeps with applied voltages of up to ± 3 V, and also with the power off,

suggesting nonvolatile WORM electronic memory characteristics. An ON/OFF current ratio of more than 10^3 , which can guarantee a low misreading rate when the voltage is controlled precisely, was achieved in this BHJ device. **Figure 3b** shows no significant degradation in either the ON state or the OFF state during the entire measuring process, suggesting good device stability. As shown in **Figure 3c**, both the ON and OFF states were insensitive to read cycles, even when more than 10^6 read cycles (pulse width = 10 μs , pulse period = 20 μs) were applied to the device. In contrast to the BHJ device, the $\text{ITO}/\text{CH}_3\text{NH}_3\text{PbI}_3/\text{Al}$ device did not exhibit any memory effect (**Figure 3d**). More precisely, this device showed only conductor characteristics under the same measurement conditions. The current-voltage characteristics of the $\text{ITO}/\text{PVK}/\text{Al}$ device were shown in **Figure 3e**. During the forward and reverse biased sweeps with an applied voltage up to ± 3 V, the device remains in the single low-conductivity state.

The switching mechanism for the bistable electrical behavior in nanoparticles/electroactive polymer-based devices has been well-explored.²⁴⁻²⁶ In our device, the bistable behavior can be attributed to an electric field-induced electron transfer from PVK to $\text{CH}_3\text{NH}_3\text{PbI}_3$. The electric field across the active layer will increase with the applied voltage. At the switching threshold voltage, the external electric field is high enough for the electron transfer between the PVK donor and the perovskite acceptor in the active layer, creating conductive film. The device is thus switched from the OFF state to the ON state. The negative charges on the perovskite are stable and prevented from moving back even when the applied voltage is removed, resulting in the nonvolatile nature of the device. When a reverse (positive) bias is applied to the device, the applied electric field is opposed by the built-in electric field associated with the thin film. The built-in electric field will prevent the trapped electrons from being extracted, and the device remains in the high conductivity state, characteristic of the behavior of a WORM memory.

To gain insights into the switching mechanism of this BHJ memory device mentioned above, *in-situ* C-AFM measurements were carried out to reveal the interesting filamentary nature of the $\text{CH}_3\text{NH}_3\text{PbI}_3$:PVK film upon being subject to voltages. As a variation of AFM and scanning tunneling microscopy, C-AFM, which uses electrical current to construct the surface profile of the studied sample, can be used to reveal electrical field-induced surface morphological changes *in situ*. In our study, a Pt-coated conductive AFM tip was used as a movable electrode that could be positioned with nanometer-scale precision and a controlled nanonewton-range force.²⁷ From **Figure 4a**, one can see that in the high resistance state (i.e., OFF state) only very low current (<1 nA) is observed at -0.5 V. When the applied voltage was changed from -0.5 V to -2 V, the device transitioned from the OFF state to the ON state. In this stage the high conductive regions (about 5 nA) appear in C-AFM current map (**Figure 4b**) due to the electric-field-induced intermolecular charge transfer (ICT) effect between PVK and $\text{CH}_3\text{NH}_3\text{PbI}_3$, and the possible conformational ordering of the PVK side-chains/backbone^{28,29} under an applied bias voltage. The diameters of the conductive areas vary from about 10 nm to 25 nm. Electrical

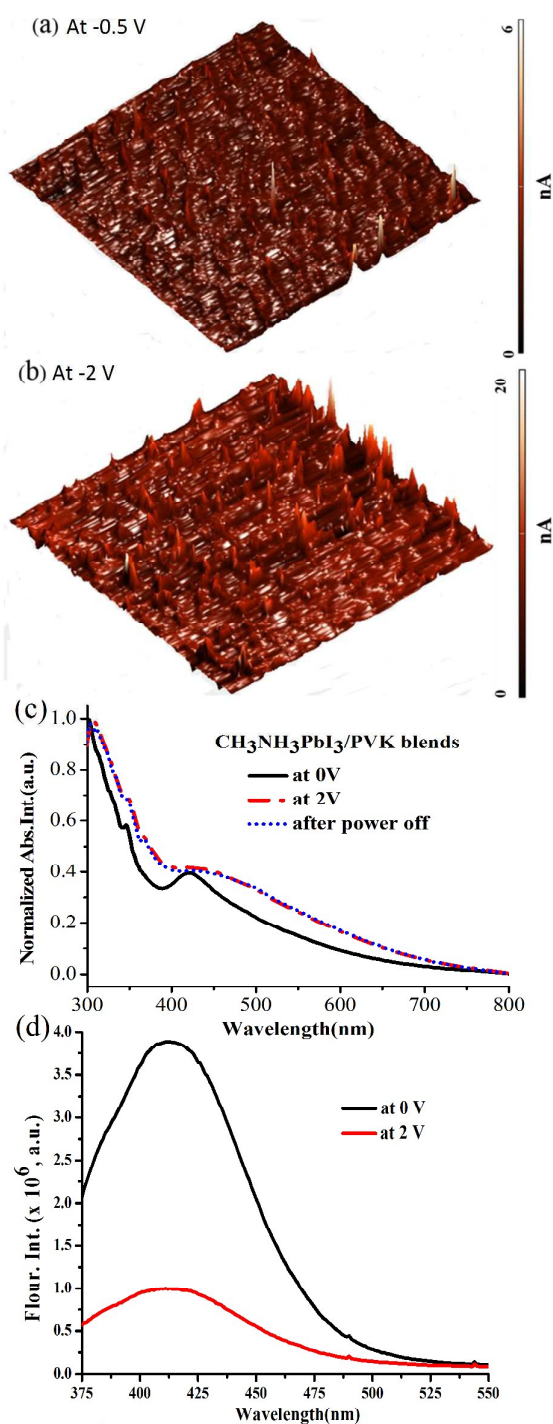


Figure 4. (a,b) C-AFM current maps of the $\text{CH}_3\text{NH}_3\text{PbI}_3/\text{PVK}$ thin film with a scanning size of $0.35 \times 0.35 \text{ mm}^2$ upon being subject to voltage. A device with a configuration of Si/Pt/ $\text{CH}_3\text{NH}_3\text{PbI}_3/\text{PVK}/\text{Pt}$ was used for C-AFM measurements; (c) UV/Vis absorption spectra of the $\text{CH}_3\text{NH}_3\text{PbI}_3/\text{PVK}$ thin film; and (d) Fluorescence spectra of the $\text{CH}_3\text{NH}_3\text{PbI}_3/\text{PVK}$ thin film. $\lambda_{\text{ex}} = 365 \text{ nm}$

current would flow through them preferentially once these highly conductive regions form. Other regions of the film were, however, no longer subject to the applied field, and would not undergo any changes in physicochemical properties.

Interestingly, after a voltage of 2 V was applied to the $\text{CH}_3\text{NH}_3\text{PbI}_3/\text{PVK}$ film on the ITO substrate, its absorption spectrum (Figure 4c) was found to shift to the red by $\Delta\lambda = 4 \text{ nm}$, followed by considerable broadening of the absorption spectrum owing to the electric-field-induced ICT³⁰ interaction between the PVK donor³¹ and the perovskite acceptor.^{32,33} The difference in LUMO levels between PVK (LUMO: -2.2 eV) and $\text{CH}_3\text{NH}_3\text{PbI}_3$ (LUMO: -3.9 eV) is much greater than 0.3 eV, implying that almost 100% charge transfer from PVK to $\text{CH}_3\text{NH}_3\text{PbI}_3$ can easily occur in such a system. After the power had been switched off for several minutes, the observed absorption spectrum was the same as that obtained at 2 V. This result suggests that electric-field-induced electronic structural changes remain even when the power is off, which will favor retention of the separated/trapped charge carriers in the BHJ memory device. And more, by using 365 nm excitation light (which is selectively excited the PVK entity), we measured the steady-state fluorescence spectra of the $\text{CH}_3\text{NH}_3\text{PbI}_3/\text{PVK}$ film before and after the applied voltage (Figure 4d). In the high resistance state (at 0 V), the film exhibited a strong emission peak at 413 nm. After the voltage of 2 V was applied to the film, a significant fluorescence quenching was observed. This quenching process is likely due to the electron transfer process from PVK to $^1\text{CH}_3\text{NH}_3\text{PbI}_3^*$. In addition, it was also found that the energy bandgap of $\text{CH}_3\text{NH}_3\text{PbI}_3$ as electron acceptor (1.5 eV) is smaller than that of PVK as electron donor (3.5 eV), this implying that the energy transfer between PVK and $\text{CH}_3\text{NH}_3\text{PbI}_3$ can also simultaneously occur in the low resistance state (i.e., ON state).

Conclusions

It has been demonstrated that the as-fabricated ITO/ $\text{CH}_3\text{NH}_3\text{PbI}_3/\text{PVK}/\text{Al}$ BHJ device shows a promising nonvolatile WORM memory effect with a turn-on voltage of about -1.57 V and an ON/OFF current ratio in excess of 10^3 . The ON state can withstand a constant voltage stress of -1 V for 10^4 s and 10^6 read cycles at -1 V under ambient conditions. In contrast, both the ITO/ $\text{CH}_3\text{NH}_3\text{PbI}_3/\text{Al}$ and ITO/ PVK/Al devices did not exhibit any memory behavior. The electric-field-induced ICT effect between $\text{CH}_3\text{NH}_3\text{PbI}_3$ and PVK, and possible conformational ordering of the PVK side-chains/backbone under an applied bias voltage, may cause the electrical conductivity switching and WORM effect in the reported BHJ device. With the advantages conferred by the bulk heterojunctions,²⁰ organometallic halide perovskite-based polymer BHJ devices hold great promise for the next generation of information storage applications.

The authors are grateful for the financial support of the National Natural Science Foundation of China (51333002,

21074034, 21404037), Research Fund for the Doctoral Program of Higher Education of China (20120074110004), and the Fundamental Research Funds for the Central Universities (WJ1514311).

Notes and references

- (1) D. Weber. *Naturforsch*, 1978, **33b**, 862.
- (2) D. Weber. *Naturforsch*, 1978, **33b**, 1443.
- (3) A. Kojima, K. Teshima, Y. Shirai, and T. Miyasaka. *J. Am. Chem. Soc.*, 2009, **131**, 6050.
- (4) F. D. Angelis. *Acc. Chem. Res.*, 2014, **47**, 3349.
- (5) W. Wang, M.O. Tadé and Z. Shao. *Chem. Soc. Rev.*, 2015, **44**, 5371.
- (6) H.S. Jung and N.-G. Park. *Small*, 2015, **11**, 10.
- (7) S. Shi, Y. Li, X. Li and H. Wang. *Mater. Horiz.*, 2015, **2**, 378.
- (8) J.-H. Im, C.-R. Lee, J.-W. Lee, S.-W. Park and N.-G. Park. *Nanoscale*, 2011, **3**, 4088.
- (9) F. Hao, C. C. Stoumpos, R. P. H. Chang and M. G. Kanatzidis. *J. Am. Chem. Soc.*, 2014, **136**, 8094.
- (10) H.-S. Kim, C.-R. Lee, J.-H. Im, K.-B. Lee, T. Moechl, A. Marchioro, S.-J. Moon, R. Humphry-Baker, J.-H. Yum, J. E. Moser, M. Grätzel, and N.-G. Park. *Sci. Rep.*, 2012, **2**, 591.
- (11) G. Xing, N. Mathews, S. Sun, S. S. Lim, Y.M. Lam, M. Grätzel, S. Mhaisalkar and T. C. Sum. *Science*, 2013, **342**, 344.
- (12) S. D. Stranks, G. E. Eperon, G. Grancini, C. Menelaou, M. J. P. Alcocer, T. Leijtens, L. M. Herz, A. Petrozza and H. J. Snaith, *Science*, 2013, **342**, 341.
- (13) C. C. Stoumpos, C. D. Malliakas and M.G. Kanatzidis. *Inorg. Chem.*, 2013, **52**, 9019.
- (14) W.-S. Yang, J. H. Noh, N. J. Jeon, Y. C. Kim, S. Ryu, J. Seo and S. I. Seok. *Science*, 2015, **348**, 1234.
- (15) T. Fujii, M. Kawasaki, A. Sawa, H. Akoh, Y. Kawazoe and Y. Tokura. *Appl. Phys. Lett.*, 2005, **86**, 012107.
- (16) S. C. Lee, Q. Hu, Y. J. Baek, Y. J. Choi, C. J. Kang, H. H. Lee and T. S. Yoon. *J. Appl. Phys.*, 2013, **114**, 064502.
- (17) M. Li, F. Zhuge, X. Zhu, K. Yin, J. Wang, Y. Liu, C. He, B. Chen and R. W. Li. *Nanotechnology*, 2010, **21**, 425202.
- (18) E. J. Yoo, M. Lyu, J.-H. Yun, C. J. Kang, Y. J. Choi and L. Wang, *Adv. Mater.*, 2015, DOI: 10.1002/adma.201502889.
- (19) C. J. Brabec, N. S. Sariciftci and J. C. Hummelen. *Adv. Funct. Mater.*, 2001, **11**, 15.
- (20) A.J. Heeger. *Adv. Mater.*, 2014, **26**, 10.
- (21) V. Dyakonov. *Phys. E (Amsterdam)* 2002, **14**, 53.
- (22) L.L. Wang, C. McCleese, A. Kovalsky, Y.X. Zhao and C. Burda. *J. Am. Chem. Soc.*, 2014, **136**, 12205.
- (23) Y.M. Xiao, G.Y. Han, Y.Z. Chang, Y. Zhang, Y.P. Li and M.Y. Li. *J. Power Sources*, 2015, **286**, 118.
- (24) J. Ouyang, C. Chu, C. R. Szmada, L. Ma And Y. Yang, *Nature Mater.* 2004, **3**, 918.
- (25) R. J. Tseng, J. Huang, J. Ouyang, R. B. Kaner, Y. Yang, *Nano Lett.*, 2005, **5**, 1077.
- (26) T. Cai, B. Zhang, Y. Chen, C. Wang, C. X. Zhu, K. Neoh, and E. T. Kang, *Chem. Eur. J.* 2014, **20**, 2723.
- (27) J. M. Mativetsky, E. Treossi, E. Orgiu, M. Melucci, G. P. Veronese, P. Samori, V. Palermo, *J. Am. Chem. Soc.* 2010, **132**, 14130.
- (28) S. Liu, Q. Chen, Y. Chen, B. Zhang, H. Liu, C. Peng and Y. Hu. *Macromolecules*, 2014, **47**, 373.
- (29) X.-D. Zhuang, Y. Chen, G. Liu, B. Zhang, K.-G. Neoh, E.T. Kang, C.-X. Zhu and Y. X. Li. *Adv. Funct. Mater.*, 2010, **20**, 2916.
- (30) B. Zhang, Y. L. Liu, Y. Chen, K. G. Neoh, Y. X. Li, C. X. Zhu, E. S. Tok and E. T. Kang, *Chem. Eur. J.* 2011, **17**, 10304.
- (31) Y. Chen, Z. Huang and R. Cai, *J. Polym. Sci. Part B: Polym. Phys.* 1996, **34**, 631.
- (32) P. Nagarjuna, K. Narayanaswamy, T. Swetha, G. H. Rao, S. P. Singh and G.D. Sharma, *Electrochim. Acta* 2015, **151**, 21.
- (33) D. Zhao, M. Sexton, H.-Y. Park, G. Baure, J.C. Nino and F. So, *Adv. Energy Mater.* 2015, **5**, 1401855.

Graphical Abstract- DT-COM-10-2015-003969

High-Efficiency Bulk Heterojunction Memory Devices Fabricated Using Organometallic Halide Perovskite:Poly(*N*-vinylcarbazole) Blend Active Layers

Cheng Wang, Yu Chen*, Bin Zhang, Shanshan Liu, Qibin Chen, Yaming Cao, Sai Sun,

The as-fabricated ITO/CH₃NH₃PbI₃:PVK/Al bulk heterojunction device exhibited a nonvolatile write-once read-many-times memory effect, with a maximum ON/OFF current ratio exceeding 10³ and a turn-on voltage of -1.57 V.

